Chapter 3. Gas Source Molecular Beam Epitaxy of Compound Semiconductors

Academic and Research Staff

Professor Leslie A. Kolodziejski, Dr. Irina Mnushkina, Dr. Gale S. Petrich

Graduate Students

Joseph F. Ahadian, Christopher A. Coronado, Jay N. Damask, Sean M. Donovan, Philip A. Fisher, Easen Ho, Jody L. House, Kan Lu

Undergraduate Students

James R. Geraci, Kuo-Yi Lim

Technical and Support Staff

Charmaine A. Cudjoe-Flanders, Angela R. Odoardi

3.1 Introduction

Current state-of-the-art epitaxial growth techniques employ various metalorganic and hydride gases to deliver constituent species to the substrate surface, particularly high vapor pressure species such as phosphorus and sulfur. Gas source molecular beam epitaxy (GSMBE) utilizes hydride gas sources and solid elemental sources. The more conventional growth approach, molecular beam epitaxy (MBE), uses only molecular beams derived from the thermal evaporation of elemental or compound solid sources.

All the research objectives described in this chapter are concerned with layered structures composed of compounds containing As and P, or Se, S, and Te. The presence of these high vapor pressure species suggests that many advantages will be attained through the fabrication of the various multilayered device structures using the gaseous source epitaxy approach.

In the chemical beam epitaxy facility at MIT, the epitaxial growth of both II-VI and III-V compound semiconductors is underway using GSMBE growth techniques. The chemical beam epitaxy laboratory consists of two gaseous source epitaxy reactors interconnected to several smaller chambers which are used for sample introduction and *in-situ* surface analysis and metalization. The multichamber epitaxy system allows for the fabrication of a large number of different heterostructures completely within a continuous ultrahigh vacuum environment. The interconnected reactors enable an additional degree of freedom in device design by providing the ability to integrate the II-VI and III-V material families into a single device. The III-V GSMBE reactor uses solid elemental sources of Ga, In, Al, Si and Be and gaseous hydride sources of arsenic and phosphorus. The II-VI reactor currently uses a solid Zn source and gaseous hydrogen selenide, in addition to a nitrogen plasma source and a solid $ZnCl_2$ source to achieve n- and p-type doping. The unique design of the II-VI reactor also allows the use of metalorganic sources. Figure 1 highlights the many heterostructure systems, based on II-VI materials, III-V materials, or on a combination of II-VI and III-V semiconductors, available for exploration. Many are currently being fabricated in our epitaxy facility.

Wide bandgap II-VI heterostructures have the potential for commercially viable short wavelength (visible to ultraviolet) optical sources for use in optical recording applications and bright emissive displays, for example. A key advance in the area of Zn chalcogenides involved the successful p-type doping of ZnSe-based semiconductors using nitrogen as the acceptor species, as first reported by Park et al.[1] The ability to dope the wide bandgap II-VIs led to the fabrication of a pn diode injection laser which operated at blue/blue-green wave-

[1] M. Park, M.B. Troffer, C.M. Rouleau, J.M. DePuydt, and M.A. Haase, "P-Type ZnSe by Nitrogen Atom Beam Doping During Molecular Beam Epitaxial Growth," *Appl. Phys. Lett.* 57: 2127-2129 (1990).
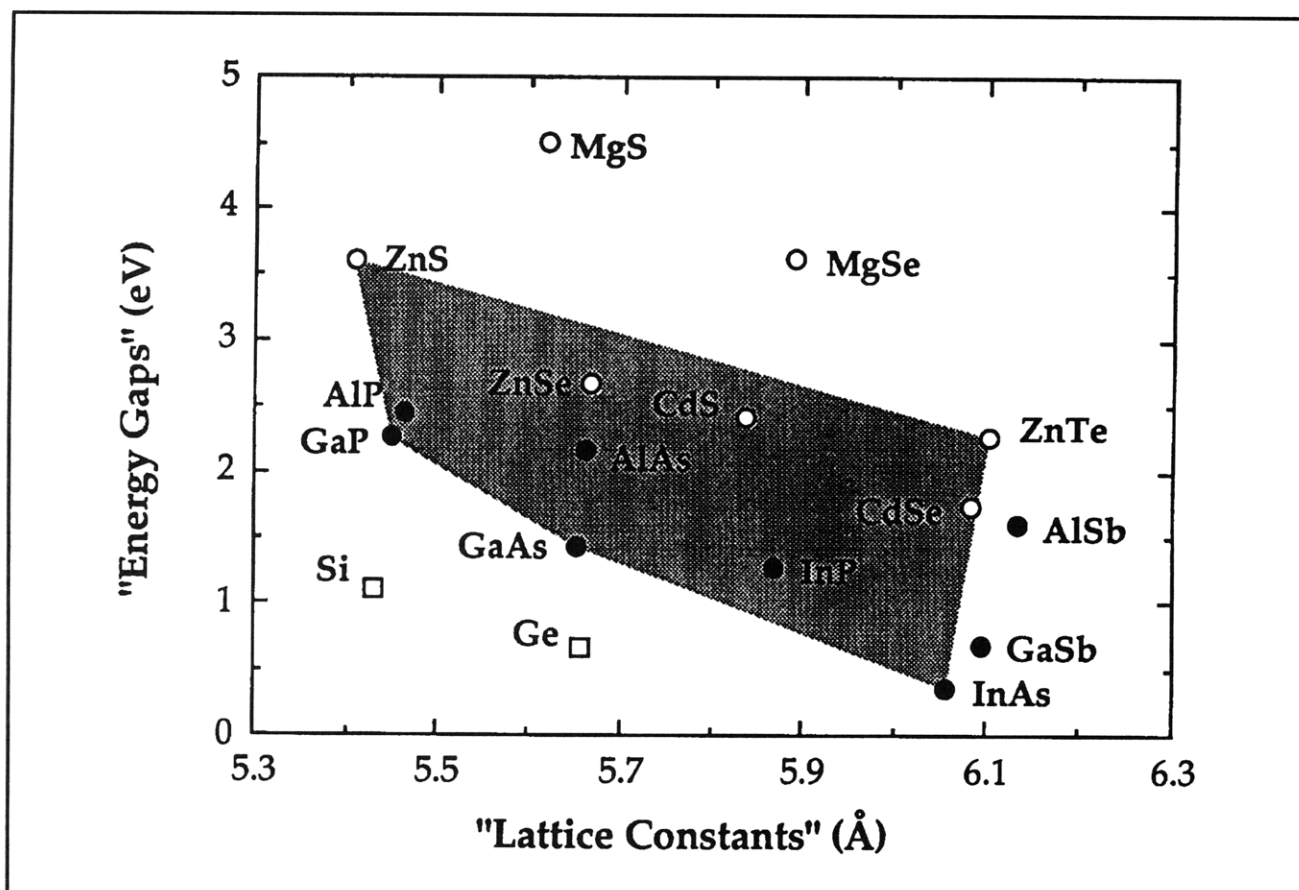
Figure 1. The shaded area highlights the many different II-VI and III-V semiconductors and the various heterostructure configurations which are available for investigation in the MIT chemical beam epitaxy laboratory.

lengths by Haase et al.[2] and H. Jeon et al.[3] The laser structures consisted of (Zn,Cd)Se narrow bandgap well layers with Zn(Se,S) cladding barrier layers, although more recent structures are composed of barrier layers of (Zn,Mg)(Se,S).[4] To minimize defect generation within the active regions of the device as well as to maximize the incorporation of the nitrogen acceptor species, the reported substrate temperatures have ranged from 150°C to 250°C. At low growth temperatures, control of the flux ratio of high vapor pressure Group II and Group VI species is very crucial and extremely difficult. By employing gas source epitaxy technologies, control of the constituent species via precision mass flow controllers (as opposed to solid source thermal effusion ovens) is anticipated to offer a solution to

the difficulties encountered in controlling the composition of ternaries and quaternaries. To address these material-related issues, we have embarked upon a II-VI-based research program which emphasizes the growth, using gas source molecular beam epitaxy, of various heterostructures which have the potential for being visible light emitters.

In the next section, we will describe our progress in the growth and doping of ZnSe using gas source molecular beam epitaxy. The II-VI effort is complemented by a program having the goal to fabricate lattice-matched epitaxial buffer layers for ZnSe that are composed of (In,Ga)P. The III-V GSMBE system is also utilized for the fabrication of (In,Ga)(As,P) waveguide devices that operate as tunable filters at 1.55 μm, which is the wavelength

2 M.A. Haase, J. Qui, J.M. DePuydt, and H. Cheng, "Blue-Green Laser Diodes," *Appl. Phys. Lett.* 59: 1272-1274 (1991).

3 Jeon, J. Ding, W. Patterson, A.V. Nurmikko, W. Xie, D.C. Grillo, M. Kobayashi, and R.L. Gunshor, "Blue-green Injection Laser Diodes in (Zn,Cd)Se/ZnSe Quantum Wells," *Appl. Phys. Lett.* 59: 3619-3621 (1991).

4 T. Okuyama, T. Miyajima, Y. Morinaga, F. Hiei, M. Ozawa, and K. Akimoto, "ZnSe/ZnMgSSe Blue Laser Diode," *Electron. Lett.* 28: 1798-1799 (1992).

of interest for optical fiber communication. New projects which are in the early stages of investigation are described at the end of the chapter and take advantage of the many capabilities available in the chemical beam epitaxy laboratory.

3.2 Gas Source Molecular Beam Epitaxy of ZnSe, ZnSe:Cl and ZnSe:N

Sponsors

Advanced Research Projects Agency
  Subcontract 284-25041
Joint Services Electronics Program
  Contract DAAL03-92-C-0001
National Center for Integrated Photonic Technology
  Contract 542-381

Project Staff

Professor Leslie A. Kolodziejski, Dr. Irina Mnushkina, Dr. Gale S. Petrich, Christopher A. Coronado, Philip A. Fisher, Easen Ho, Jody L. House, James R. Geraci, Kuo-Yi Lim

In the case of the growth of the II-VI material family, all the constituent species are high vapor pressure elements necessitating the reproducible control of effusion cells which operate at low temperatures. The difficulty in maintaining elemental effusion cells at very low temperatures ($\sim 180 - 300°C$) is eliminated by the use of mass flow controllers which precisely regulate the flow of gaseous anion species. The ZnSe-based heterostructure system has relevance to the optoelectronics community for system applications requiring optical sources operating in the green to UV spectral range. In this program, the growth and doping of ZnSe by GSMBE are investigated.

ZnSe was grown on semi-insulating, n- and p-type (001) GaAs bulk substrates using elemental Zn and gaseous H_2Se. The growth temperature ranged from 240°C to 400°C, although the majority of the films were grown at 270°C. The substrate temperature was calibrated by observing the eutectic phase transition (356°C) of 500 Å of Au that was deposited onto Ge and was continuously monitored using an optical pyrometer. The H_2Se gas flow was varied from 0.8 to 4.2 sccm and resulted in a chamber pressure of approximately 2×10^{-5} Torr during growth; the H_2Se was thermally decomposed at 1000°C. The zinc flux, as measured by a water-

cooled crystal oscillator placed in the substrate position, corresponded to a zinc deposition rate ranging from 0.5 to 2.3 Å/s. Under these conditions, the Se:Zn flux ratio ranged from 1.3:1 to 0.6:1. During the epitaxial growth process, the surface stoichiometry was monitored by observing the surface reconstruction using reflection high energy electron diffraction (RHEED). A radio frequency (RF) plasma cell was used for a source of atomic nitrogen acceptor species. The RF power to the plasma cell was varied from 100 to 500 Watts. A leak valve regulated the nitrogen gas flow, while an ionization gauge in the reactor measured the equilibrium nitrogen pressure, which ranged from 6×10^{-7} to 2×10^{-5} Torr. The ZnSe was doped n-type using a $ZnCl_2$ source having a source temperature which ranged from 150°C to 250°C. The ZnSe was grown at rates of 0.3 to 0.7 μm/hour to layer thicknesses of 1 to 4 μm.

The optical properties of the epitaxial ZnSe layers were measured by photoluminescence (PL). PL was obtained by optically exciting the samples with the 3250 Å line of a focused He-Cd laser, providing a power density of approximately 300 mW/cm². The ZnSe luminescence was analyzed with a half-meter spectrometer and a photomultiplier. Figure 2 shows the low temperature (10K) PL spectra obtained from a series of undoped ZnSe films grown under identical growth conditions, but with different substrate temperatures. For each growth temperature investigated, the PL spectrum was dominated by an intense donor-bound exciton feature having an energy of 2.798 eV and is speculated to be due to an unintentionally incorporated donor originating from the source materials. The deep level defect-related luminescence band, which is broadly centered about 2.25 eV, was at least 100-1000 times weaker in intensity than the near-bandedge features. To elucidate the presence of the defect-related luminescence, photoluminescence was also obtained at 77K. As seen in figure 3, as a function of growth temperature, the PL spectra showed that the donor-bound exciton persisted as the dominant feature. However, at the growth temperature extremes, a small amount of luminescence originating from deep levels was observed. As another indication of the high quality of the ZnSe layers, the integrated PL intensity of the near-bandedge feature was found to decrease to one-sixtieth of its 10K value as the sample temperature was increased to room temperature; room temperature luminescence was easily observed by the naked eye.
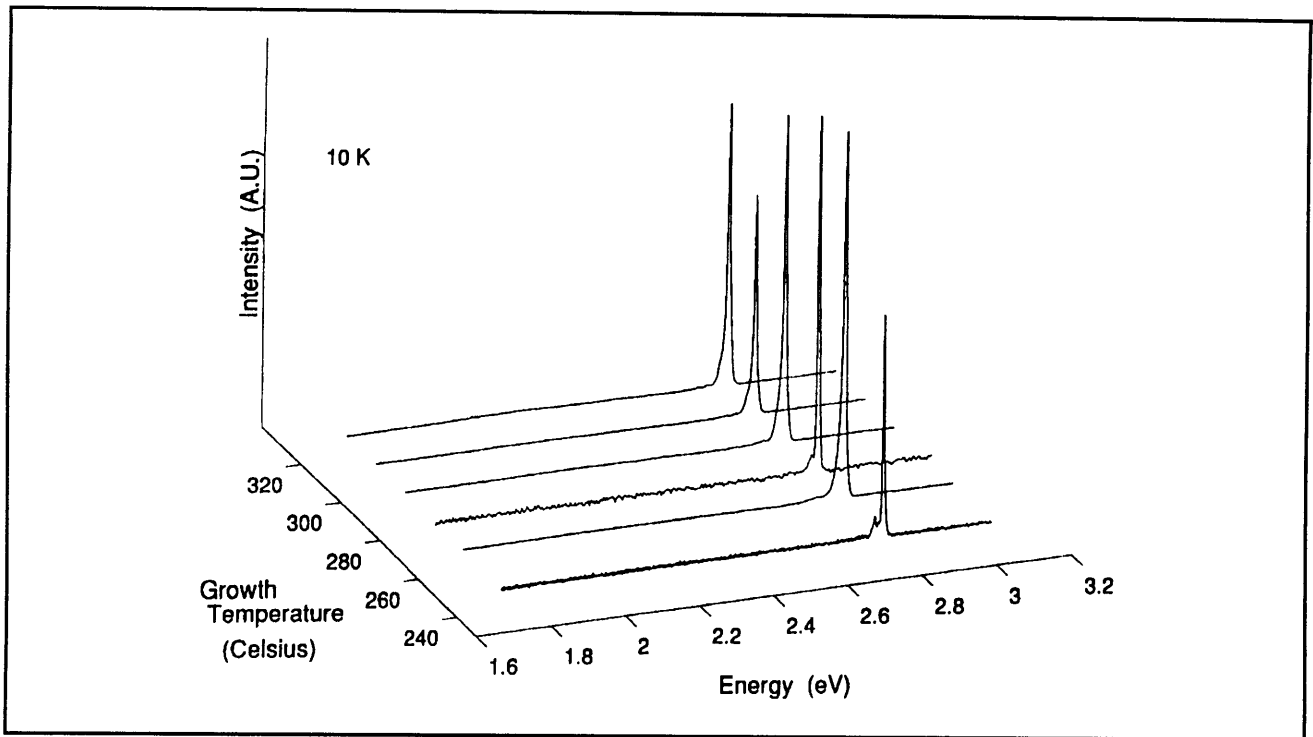
Figure 2. The 10K photoluminescence intensity as a function of energy for ZnSe epilayers grown at various substrate temperatures. The dominant donor-bound exciton had an energy of 2.798 eV. The ZnSe film that was grown at 284°C, was deposited on an (In,Ga)P buffer layer.
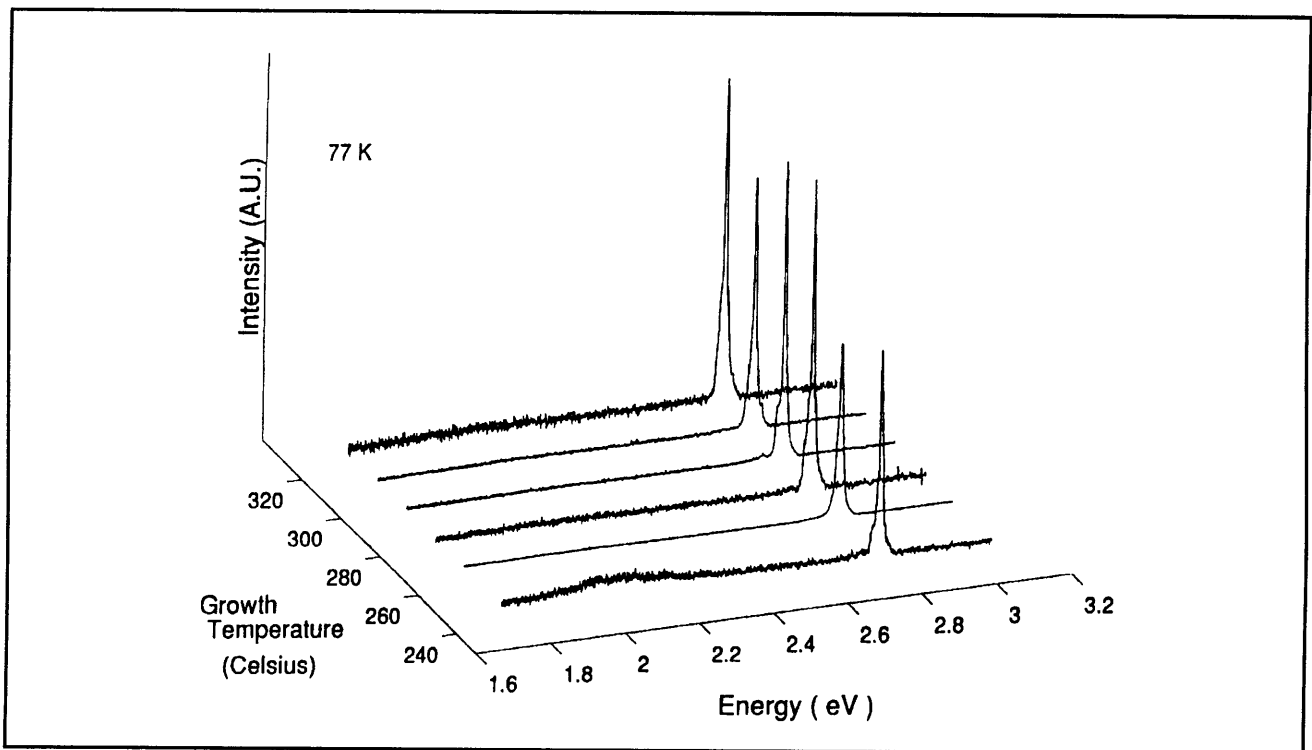

Figure 3. The 77K photoluminescence intensity as a function of energy for ZnSe epilayers grown at various substrate temperatures. The dominant donor-bound exciton has an energy of 2.787 eV. The ZnSe film that was grown at 284°C, was deposited on an (In,Ga)P buffer layer.
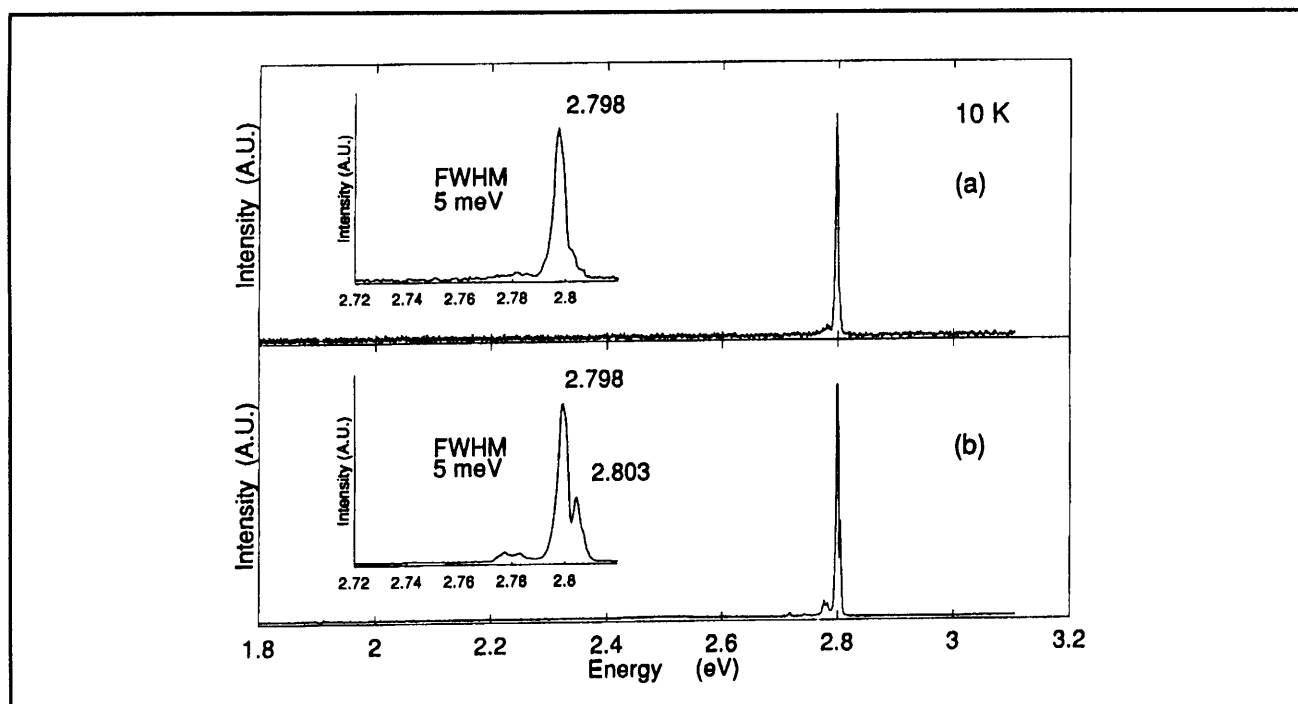
Figure 4. The 10K photoluminescence intensity as a function of energy (the inset shows a higher resolution energy scan). The spectrum in (a) reflects the PL obtained from ZnSe grown under Se-rich surface stoichiometry conditions, whereas (b) was obtained from a sample grown under conditions of Zn-rich surface stoichiometry. All other growth parameters were held constant.

During the growth, the surface stoichiometry was varied to provide either a Zn-rich or Se-rich surface by modifying the H_2Se gas flow. Changes in the RHEED pattern from a (2x1) reconstructed pattern, suggesting a Se-rich surface, to a (2x2) reconstructed pattern, suggesting a Zn-rich surface, verified the presence of a particular surface stoichiometry. The surface stoichiometry, which was maintained throughout the growth, was found to influence the near-bandedge PL features, as well as the unintentional impurity incorporation. Figure 4 compares the PL spectrum, obtained from an undoped ZnSe film grown under Se-rich surface stoichiometry (figure 4a) to a sample grown under Zn-rich surface stoichiometry (figure 4b). All other growth parameters were identical.

Regardless of the surface stoichiometry, the near-bandedge luminescence was dominated by a donor-bound exciton transition. However, an increase in the intensity of the free exciton feature (at an energy of 2.803 eV) was apparent in the undoped films grown under conditions which provide a Zn-rich surface stoichiometry. Differences in the undoped carrier concentration were also observed depending on the surface stoichiometry. Room temperature Hall effect measurements were performed on the undoped ZnSe samples with indium contacts in the Van der Paaw geometry. Films grown with a Se-rich surface

stoichiometry had free electron concentrations in the mid 10^{16} to low 10^{17} cm^{-3} range, while films grown with a Zn-rich surface stoichiometry had free electron concentrations from the mid 10^{15} to low 10^{16} cm^{-3}.

The RF plasma cell provided a source of both atomic and molecular nitrogen species, while a $ZnCl_2$ effusion cell provided a source of Cl for investigation of the p- and n-type doping, respectively, of ZnSe using the GSMBE growth technique. The nitrogen pressure was monitored by an ionization gauge within the reactor (prior to insertion of the H_2Se gas). The Cl doping level was controlled by the temperature of the $ZnCl_2$ effusion cell. Characterization of the doped ZnSe layers was performed using photoluminescence, Nomarski microscopy, double crystal x-ray diffraction rocking curves, secondary ion mass spectroscopy (SIMS), and capacitance-voltage (C-V) measurements. The observed structural characteristics were similar to the undoped layers. Specifically, the surface remained featureless as examined by Nomarski microscopy for all doping conditions explored thus far; the (400) peak of the x-ray rocking curves exhibited typical full width at half maximum (FWHM) ranging from 175 to 200 arc seconds.

Low temperature PL was used to optically characterize both the nitrogen- and chlorine-doped ZnSe
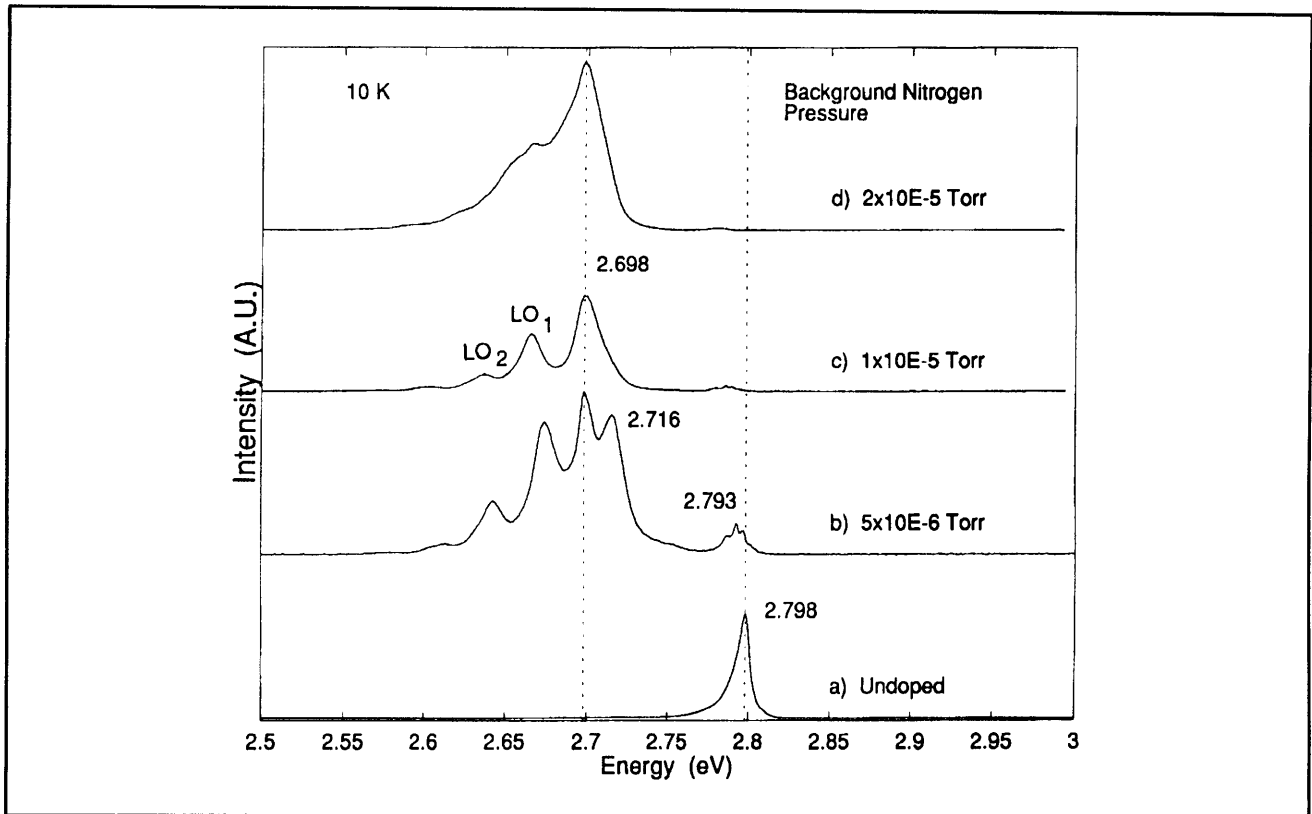
Figure 5. The 10K photoluminescence intensity as a function of energy for various nitrogen gas flows. (b)-(d) The nitrogen flow was increased to vary the incorporation of nitrogen acceptor species. The PL obtained from undoped ZnSe (a) is shown for comparison.

epilayers. The photoluminescence obtained from ZnSe:N layers are shown in figure 5. In this figure, the 10K spectra are compared for samples grown under identical growth conditions; however, the nitrogen gas flow was systematically increased to enhance the incorporation of acceptors into the lattice. Figure 5 illustrates that the characteristic PL features of the ZnSe:N films were strongly dependent on the degree of nitrogen incorporation. The growth conditions for the series of films in figure 5 were as follows: a 270°C calibrated substrate temperature, a Se-rich surface stoichiometry, and a constant RF power of 100 Watts for the plasma source. From the comparisons of the dominant transitions observed in the 10K PL, we deduced that the nitrogen concentration increased with higher nitrogen gas flow, as expected. For the sample grown with the lowest nitrogen flow, shown in figure 5b, the near-bandedge transitions were dominated by the neutral N acceptor peak at 2.793

eV. (PL obtained from an undoped sample is shown for reference in figure 5a.)

The free electron-to-acceptor transition (FA) was present at 2.716 eV indicating a nitrogen acceptor binding energy of 109 meV, assuming a 10 K bandgap energy of 2.825 eV.[5] The donor-to-acceptor-pair (DAP) transition peak at 2.698 eV and the associated LO phonon replicas were also detected. Further increases in the nitrogen flow resulted in a spectrum dominated by the FA and DAP transitions (and their LO phonon replicas), as shown in figure 5c. At the highest nitrogen gas flows investigated (figure 5d), the FA transition disappeared, while the DAP and phonon replicas merged into a single broad feature. Similar PL spectra for variations in the nitrogen incorporation for ZnSe:N grown by MBE were observed by Ohkawa et al.[6] In addition, for a given doping condition, a Zn-rich surface stoichiometry appeared to

---

[5] P.J. Dean, D.C. Herbert, C.J. Werkhoven, B.J. Fitzpatrick, and R.N. Bhargava, "Donor Bound Exciton Excited States in Zinc Selenide," *Phys. Rev. B* 23: 4888-4901 (1981).

[6] K. Ohkawa, T. Karasawa and T. Mitsuyu, "Characteristics of p-type ZnSe Layers Grown by Molecular Beam Epitaxy with Radical Doping," *Jpn. J. Appl. Phys.* 30: L152-L155 (1991).

incorporate the nitrogen species more effectively, since the PL spectrum from a Zn-rich surface stoichiometry exhibits a single broad DAP transition, while the spectrum from a Se-rich surface stoichiometry consisted of multiple, easily distinguished DAP (and LO phonon replicas) transitions. The PL spectra from 2 μm Cl-doped ZnSe epilayers consisted of a single donor-bound exciton transition at 2.795 eV. By comparing various samples, the intensity of the donor-bound exciton transition was found to increase linearly as the Cl concentration was increased from 2×10^{16} to 2×10^{17} cm^{-3}. The free electron carrier concentration was determined by room temperature Hall measurements and correlated to atomic incorporation levels obtained by SIMS measurements.[7]

The incorporation level of nitrogen in the ZnSe:N samples was also determined by secondary ion mass spectroscopy. A nitrogen-implanted ZnSe standard was used to calibrate the nitrogen concentration, resulting in a detection limit that was estimated to be approximately 10^{17} cm^{-3}. For growth under Se-rich surface stoichiometry, the measured nitrogen concentration ranged from below the detection limit of the SIMS apparatus ($< 10^{17}$ cm^{-3}) to 4.0×10^{18} cm^{-3}. In comparison, samples grown under Zn-rich conditions had nitrogen concentrations ranging from 2×10^{17} to 5.0×10^{18} cm^{-3}. These results agreed with the qualitative comparisons of the PL features obtained from the samples that were grown under Zn-rich and Se-rich surface stoichiometries.

The ZnSe:N films were electrically characterized by C-V measurements due to the difficulty in forming an ohmic contact to p-type ZnSe. The measurements were made using Cr/Au Schottky contacts in a ring-dot electrode configuration at a measurement frequency of 1 MHz. The devices were typically 200 μm dots with a 20 μm wide separation between the center dot and the outer ground plane. Thus far, net acceptor concentrations (N_A–N_D) of 1.0×10^{17} cm^{-3} have been measured and correspond to a nitrogen concentration of 1.5×10^{18} cm^{-3} (as measured by SIMS).

3.2.1 Publications

Coronado, C.A., E. Ho, and L.A. Kolodziejski. "Effect of Laser on MOMBE of ZnSe Using Gaseous and Solid Sources." *J. Crystal Growth* 127: 323-326 (1993).

Coronado, C.A., E. Ho, P.A. Fisher, J.L. House, K. Lu, G.S. Petrich, and L.A. Kolodziejski. "P-Type Doping of ZnSe Using a Nitrogen Plasma during GSMBE." Paper presented at the Electronic Materials Conference, Santa Barbara, California, June 21-23, 1993.

Coronado, C.A., E. Ho, P.A. Fisher, J.L. House, K. Lu, G.S. Petrich, and L.A. Kolodziejski. "Gas Source Molecular Beam Epitaxy of ZnSe and ZnSe:N." *J. Electron. Mater.* 23: 269-274 (1994).

Ho, E., C.A. Coronado, and L.A. Kolodziejski. "Elimination of Surface Site Blockage Due to Ethyl Species in MOMBE of ZnSe." *J. Electron. Mater.* 22(5): 473-478 (1993).

Ho, E., C.A. Coronado, and L.A. Kolodziejski. "Photo-Assisted Chemical Beam Epitaxy of II-VI Semiconductors." In *Beam-Solid Interactions: Fundamentals and Applications.* Eds. M. Nastasi, L.R. Harriott, N. Herbots, and R.S. Averback. Pittsburgh: Materials Research Society, 1993, vol. 279, pp. 635-644.

Ho, E., P.A. Fisher, J.L. House, C.A. Coronado, G.S. Petrich, L.A. Kolodziejski, M.S. Brandt, and N.M. Johnson. "P- and N-Type Doping of ZnSe Using GSMBE." Spring Meeting of the Materials Research Society, San Fransisco, California, April 4-8, 1994.

Ho, E., C.A. Coronado, P.A. Fisher, J.L. House, K. Lu, G.S. Petrich, and L.A. Kolodziejski. "Gaseous Source Epitaxy of ZnSe: MOMBE and GSMBE." Paper presented at the International Conference on Chemical Beam Epitaxy and Related Growth Techniques, Nara, Japan, July 23-25, 1993.

Thesis

House, J.L. *Optical Characterization of ZnSe by Photoluminescence.* S.M. thesis, Dept. of Electr. Eng. and Comput. Sci., MIT, 1994.

---

[7] SIMS performed in collaboration with Dr. Noble Johnson, Xerox Palo Alto Research Center, Palo Alto, California.
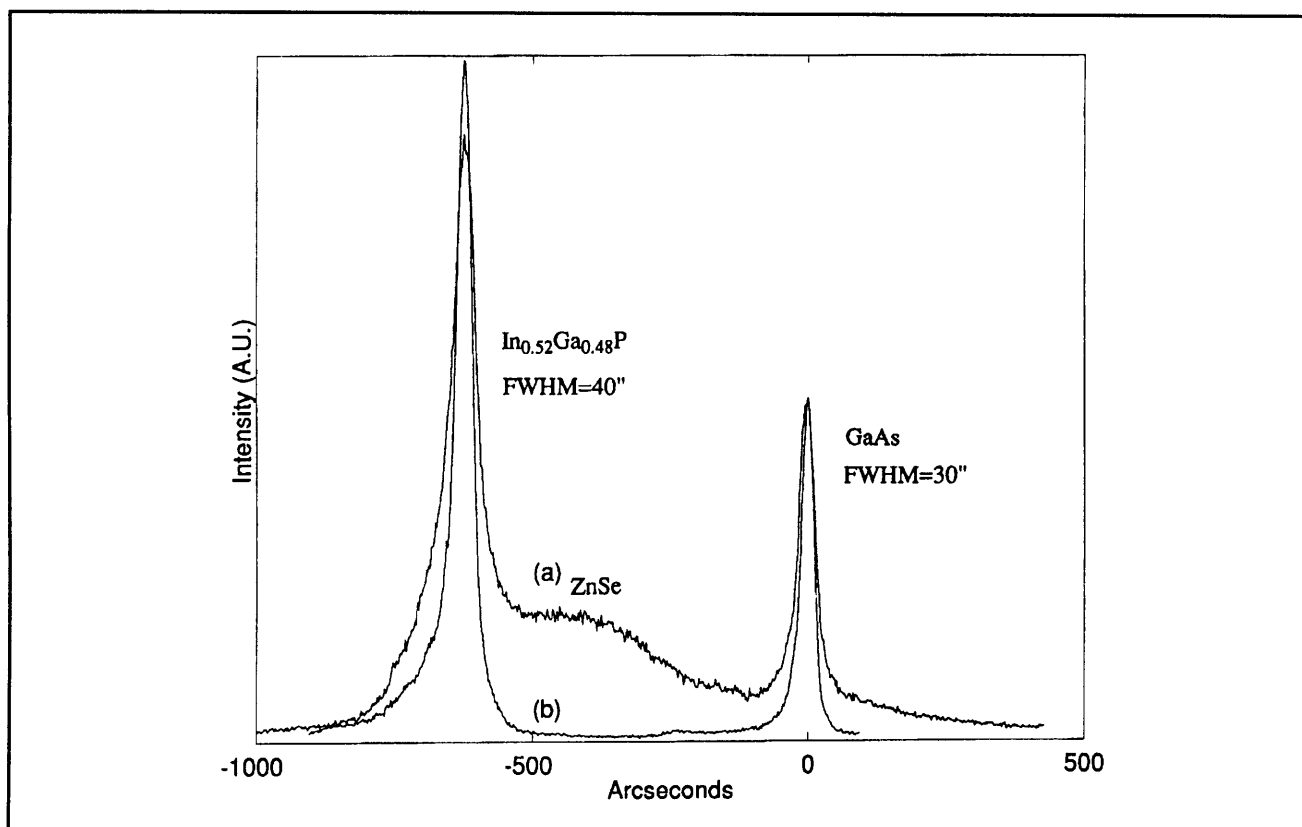
Figure 6. (a) (400) x-ray rocking curve obtained from a 1.1 μm ZnSe film grown on 4.3 μm (In,Ga)P. The residual strain between the GaAs substrate and the (In,Ga)P buffer layer is $\Delta a/a = 0.15$ percent. (b) The (In,Ga)P (400) x-ray rocking curve obtained after the ZnSe had been selectively etched. The peak of the GaAs substrate feature has been shifted to 0 arc seconds for clarity.

3.3 Novel Epitaxial III-V Buffer Layers for Wide Bandgap II-VI Visible Sources

Sponsors

Project Staff

Professor Leslie A. Kolodziejski, Dr. Gale S. Petrich, Christopher A. Coronado, Philip A. Fisher, Easen Ho, Jody L. House, Kan Lu, Kuo-Yi Lim

The ZnSe-based material system, in which (Zn,Mg)(S,Se) barrier layers and (Zn,Cd)Se well layers are used, offers the ability to fabricate a multitude of heterostructure devices capable of emitting light throughout the entire visible region. A significant device bottleneck, however, is the lack of large area, high quality bulk II-VI substrates. As a result, the II-VI devices are grown on III-V substrates which can potentially lead to the presence of appreciable lattice-mismatch strain within the II-VI layer. The detrimental effects of lattice-mismatch constrain the present state-of-the-art blue-green semiconductor lasers to be designed to be fully strained, such that the structures are pseudomorphic to bulk GaAs.[8] The use of (In,Ga)P epitaxial buffer layers as an "alternate substrate" enables the (In,Ga)P lattice constant to be continuously varied from that of ZnS (GaP) to roughly that of $Zn_{0.5}Cd_{0.5}Se$ (InP) (see figure 1). By matching the lattice constant of the III-V "alternative substrate" to the II-VI structure, the strain is minimized in the II-VI device layers, and the misfit dislocations can be engineered to remain primarily near the (In,Ga)P/GaAs interface, as opposed to the ZnSe/(In,Ga)P interface. The use of these novel

---

8 T. Okuyama, T. Miyajima, Y. Morinaga, F. Hiei, M. Ozawa, and K. Akimoto, "ZnSe/ZnMgSSe Blue Laser Diode," *Electron. Lett.* 28: 1798-1799 (1992).

buffer layers is anticipated to lead to an improvement in the device's performance, as well as to provide greater flexibility in II-VI laser design to achieve shorter wavelengths of blue emission. Additional benefits are expected to be derived (1) from the chemical differences which exist between the ZnSe and (In,Ga)P, as compared to GaAs, for future device processing, and (2) by utilizing various band structure engineering techniques to provide a graded transition in the valence band discontinuity present between GaAs and ZnSe which is necessary for optimized electronic transport.

The III-V layers were grown using GSMBE in a dedicated reactor. The (In,Ga)P buffer layers were grown at 450°C (on a 0.5 μm homoepitaxial GaAs buffer layer), where the substrate temperature was calibrated using the melting point of InSb (525°C). Elemental effusions cells containing In and Ga, in addition to PH_3, which is cracked at 900°C, were used as sources. The (In,Ga)P surface exhibited a sharp (2x1) surface reconstruction during growth, as observed by RHEED. During the initial minutes following nucleation, RHEED intensity oscillations were observed and were used to estimate the alloy composition in real time. The precise alloy composition was determined by (400) and (511) reflections of high resolution x-ray diffraction rocking curves. The thicknesses of the (In,Ga)P buffer layers were (1) estimated from the Group III fluxes, (2) obtained from RHEED oscillations which indicate the growth rate, and (3) subsequently measured by a profilometer following the selective removal of the ZnSe and (In,Ga)P by chemical etching. At the completion of the (In,Ga)P buffer layer, the surface was coated *in situ* with amorphous As by lowering the substrate temperature to below 100°C in an arsenic-rich environment (obtained by using a cracked AsH_3 flux). The samples were then transferred *ex situ* to the II-VI GSMBE reactor. The amorphous As was thermally desorbed from the (In,Ga)P buffer layers at approximately 270°C. During the nucleation of ZnSe on the (In,Ga)P epitaxial surface, a streaky RHEED pattern was observed in most cases, and persisted throughout the entire growth of the ZnSe layer. However, a bulk diffraction pattern was observed from the ZnSe during the initial stages of growth, if the temperature of the (In,Ga)P buffer layer was increased to temperatures nearing 400°C during the As desorption process. Excessive phosphorus evaporation is speculated to have occurred at the higher As desorption temperatures and contributed to the three dimensional nucleation behavior of ZnSe on (In,Ga)P.

The ZnSe/(In,Ga)P/GaAs heterostructures were examined by high resolution (four and double crystal) x-ray diffraction. The (In,Ga)P compositions were calculated using both the (400) and the (511) rocking curves and correlated with the RHEED intensity oscillations. The information derived from the (511) rocking curves indicated that the (In,Ga)P films having thicknesses of roughly 1 μm were pseudomorphic to the GaAs substrate, and that even films having thicknesses greater than 4 μm were only partially relaxed. Figure 6a shows the (400) x-ray rocking curve obtained from the ZnSe/(In,Ga)P/GaAs heterostructure containing a 4.3 μm $In_{0.52}Ga_{0.48}P$ buffer layer. Figure 6b shows the identical structure following the removal of the 1.1 μm ZnSe layer by selective etching. The FWHM for each of the peaks from the III-V layers are 30 arc seconds for GaAs and 40 arc seconds for the (In,Ga)P. The (511) rocking curves for this structure indicated that the (In,Ga)P was not fully relaxed, but still contained approximately 0.11 percent lattice mismatch between the ZnSe and the (In,Ga)P. According to the (511) rocking curves, the composition of the (In,Ga)P film was such that when fully relaxed, the in-plane lattice constant would be the same as that of ZnSe. The width of the (400) ZnSe peak reflects the presence of dislocations at the ZnSe/III-V heterointerface due to the presence of the lattice-mismatch which still remains.

Comparisons of the surface morphology using optical Nomarski microscopy and scanning electron microscopy (SEM), indicated that the ZnSe films grown on the (In,Ga)P buffer layers (and on the bulk GaAs substrates) were featureless at SEM magnifications as high as 12,000 times. For epitaxial buffer layers of (In,Ga)As lattice-matched to ZnSe, the III-V surface was reported to have significant cross hatching due to lattice relaxation.[9] Similar surface features have been observed for $In_xGa_{1-x}P$ films which have been grown at In compositions (x = 0.55), which when fully relaxed, would have a lattice constant greater than the in-plane lattice constant of ZnSe. For In compositions of x = 0.55, the layers were only partially relaxed, but exhibited in-plane lattice constants lattice-matched to ZnSe; in this case, the (In,Ga)P surface appeared cross-hatched. In addition, for a given In composition, growth conditions using a higher growth temperature (500°C) resulted in a cross-hatched surface.

The optical properties of the ZnSe films were measured using PL spectroscopy. The 10K PL spectra

---

9 Private communication with R.L. Gunshor, Purdue University, LaFayette, Indiana.

of the ZnSe on the pseudomorphic (In,Ga)P buffer layers, or on bulk GaAs substrates, were dominated by the luminescence attributed to transitions associated with donor-bound excitons. Defect-related luminescence originating from mid-bandgap deep levels was not observed. However, the photoluminescence from ZnSe grown on the partially-relaxed (In,Ga)P buffer layers contained features identified as those due to both donor-bound excitons (2.795 eV) and free excitons (2.803 eV) having roughly the same intensity (as can be seen in figure 7). For the samples examined, which have a very high degree of purity, the Y_0 (2.603 eV) and

I_v (2.775 eV) transitions were also detected. Both the Y_0 and I_v transitions have been reported to be due to extended defects[10] which suggested that the ZnSe layer still contained defects due to lattice relaxation. The observation of the Y_0 and I_v transitions served as additional evidence that these (In,Ga)P buffer layers were only partially relaxed, whereas the ZnSe was completely relaxed (and confirmed by cross-sectional transmission electron microscopy). The transition occurring at 1.938 eV is attributed to the PL originating from the (In,Ga)P buffer layer.
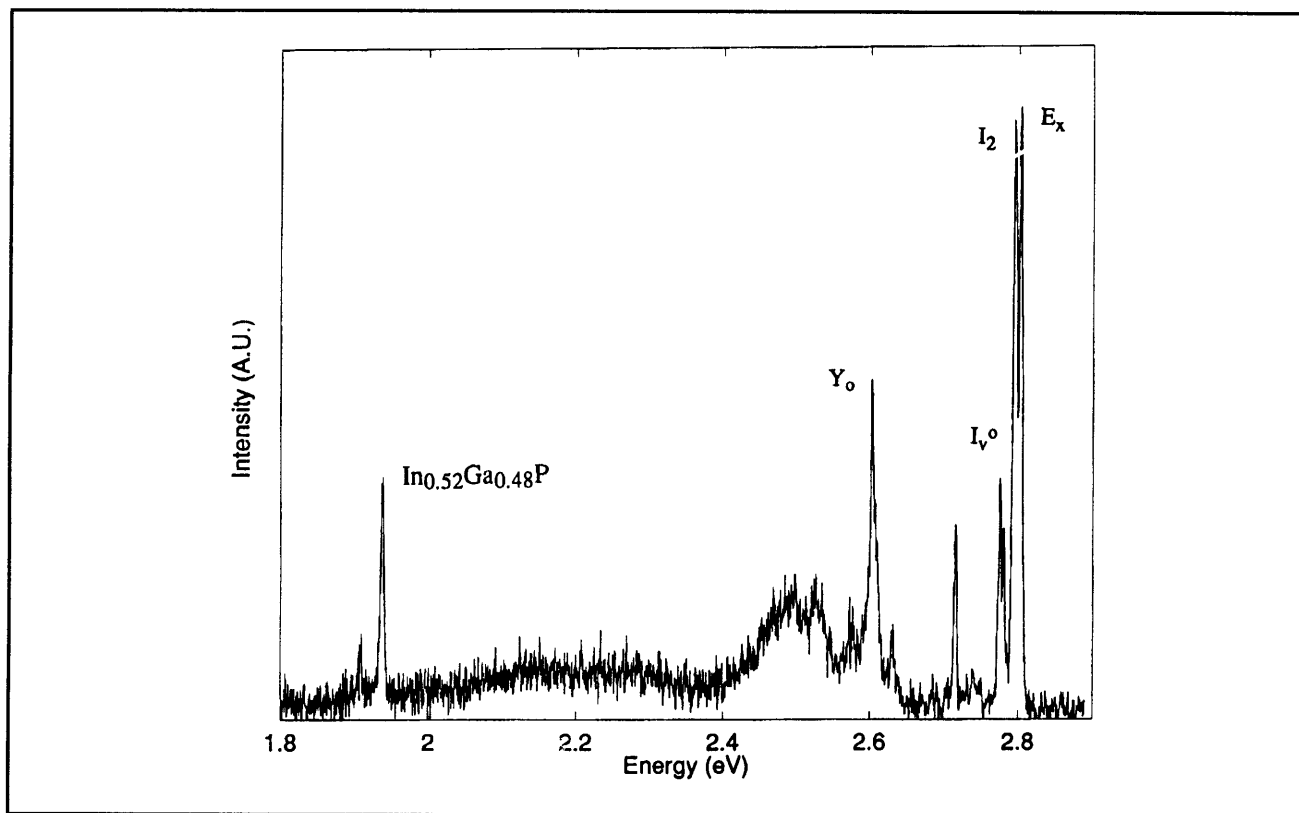

Figure 7. 10 K photoluminescence spectrum of the 1.1 μm ZnSe film grown on a partially relaxed 4.3 μm (In,Ga)P film. The feature at 1.938 eV is attributed to the photoluminescence from the (In,Ga)P buffer layer. Features at 2.803, 2.795, 2.776 and 2.603 are identified as transitions due to free excitons, donor-bound excitons, $I_v°$, and Y_0, respectively. The origin of the feature at 2.717 is unknown and under investigation. (The feature at 1.907 eV is the second harmonic of the 3250 Å line from the HeCd laser.)

10 J. Saraie, M. Matsumura, M. Tsubokura, K. Miyagawa, and N. Nakamura, "Y-line Emission and Lattice Relaxation in MBE-ZnSe and -ZnSSe on GaAs," *Jpn. J. Appl. Phys.* 28: L108-L111 (1989); K. Shahzad, J. Petruzzello, D.J. Olego, D.A. Cammack, and J.M. Gaines, "Correlation between Radiative Transitions and Structural Defects in Zinc Selenide Epitaxial Layers," *Appl. Phys. Lett.* 57: 2452-2454 (1990); J.O. Williams, A. Wright, and H.M. Yates, "High Resolution and Conventional Transmission Electron Microcopy in the Characterization of Thin Films and Interfaces Involving II-VI Materials," *J. Cryst. Growth* 117: 441-453 (1992).

Characterization by photoluminescence indicates that high quality ZnSe epilayers have been grown on (In,Ga)P buffer layers by GSMBE. However, the critical thickness of the (In,Ga)P epilayers greatly exceeded the value predicted by the Matthews and Blakeslee force balancing model (47 nm),[11] as well as by a model which uses an assumption of energy balance (3.2 μm).[12] Various techniques that induce lattice relaxation are under investigation so that we can control the selection of a specific in-plane lattice constant for heteroepitaxy. Thus far, (In,Ga)P is a promising epitaxial substrate material for the realization of devices based on ZnSe and related II-VI compounds.

3.3.1 Publications

Lu, K., J.L. House, P.A. Fisher, C.A. Coronado, E. Ho, G.S. Petrich and L.A. Kolodziejski. "GSMBE Growth of ZnSe on Novel Buffer Layers." *J. Vac. Sci. Tech. B* (1994). Forthcoming.

Lu, K., P.A. Fisher, E. Ho, J.L. House, C.A. Coronado, G.S. Petrich, and L.A. Kolodziejski. "GSMBE of ZnSe on (In,Ga)P." Spring Meeting of the Materials Research Society, San Fransisco, California, April 4-8, 1994.

Lu, K., P.A. Fisher, J.L. House, E. Ho, C.A. Coronado, G.S. Petrich, and L.A. Kolodziejski. "(In,Ga)P Buffer Layers for ZnSe-Based Visible Emitters." *J. Cryst. Growth* (1994). Forthcoming.

Thesis

Lu, K. *Lattice-Matched (In,Ga)P Buffer Layers for ZnSe Based Visible Emitters.* S.M. thesis, Dept. of Electr. Eng. and Comput. Sci., MIT, 1994.

3.4 Integrated Photonic Devices: The Channel-Dropping Filter

Sponsor

National Center for Integrated Photonic Technology
Contract 542-381

Project Staff

Professor Hermann A. Haus, Professor Leslie A. Kolodziejski, Professor Henry I. Smith, Dr. Gale S. Petrich, Jay N. Damask

The channel-dropping filter, first proposed by Professor Hermann Haus,[13] is a member of a family of integrated photonic wavelength-division multiplexers (WDM) and demultiplexers. Unlike other multiplexers which terminate and resolve an entire bit stream within one device, the channel-dropping filter can selectively add (or remove) only one wavelength channel, while the other remaining channels are left undisturbed. The property of single channel filtering offers a new degree of freedom to the WDM network architecture. Our objective is to fabricate the integrated resonant channel-dropping filter using the (In,Ga)(As,P) compound semiconductor material system.

The (In,Ga)(As,P) semiconductor system meets several of the material requirements for the fabrication and eventual implementation of the channel-dropping filter. The (In,Ga)(As,P) heterostructure system is compatible with optical communication systems operating at 1.55 μm and is lattice-matched to InP over a wide range of direct energy bandgaps ($\lambda_g \approx 0.87\ \mu$m for InP through $\lambda_g = 1.67\ \mu$m for $In_{0.53}Ga_{0.47}As$). The quaternary material system also possesses sufficiently large differences in the index of refraction for various alloy compositions, which is necessary to confine an optical mode, and the material has been reported to exhibit waveguide losses of $\leq$ 1 dB/cm.

Our current research has focused on the device design, epitaxial growth, and fabrication of passive low-loss waveguides. Vertical optical mode confinement in the waveguides is achieved by controlling the index of refraction, via the correct selection of the energy bandgap for each epitaxial layer. The energy bandgap is determined by the mole fraction of the constituent alloy elements: In, Ga, As, and P.

---

[11] J.W. Matthews and A.E. Blakeslee, "Defects in Epitaxial Multilayers: I. Misfit Dislocations," *J. Crystal Growth* 27: 118-125 (1974).

[12] R. People and J.C. Bean, "Calculation of Critical Layer Thickness Versus Lattice Mismatch for Ge_xSe_{1-x}/Si Strained-layer Heterostructures," *Appl. Phys. Lett.* 47: 322-324 (1985).

[13] H.A. Haus and Y. Lai, "Narrow-Band Optical Channel-Dropping Filter," *J. Lightwave Technol.* 10: 57-62 (1992).

The III-V-dedicated gas source molecular beam epitaxy reactor uses elemental sources for In and Ga, and gaseous hydride sources for As and P. The ratio of Group III and Group V elements determines the energy bandgap and lattice constant for a particular quaternary alloy.

Control of the alloy composition for $In_{1-x}Ga_xAs_yP_{1-y}$ is difficult due to the vastly different sticking coefficients of the Group III and Group V species. For a narrow range of growth temperature, the sticking coefficients for the indium and gallium atoms are near unity, whereas the sticking coefficients for the arsenic dimers and phosphorus dimers are less than unity, varying strongly with substrate temperature. The In/Ga flux ratio, and hence composition, is selected by the appropriate choice of the two elemental source temperatures. However, the As/P composition ratio cannot be similarly established. In competition for surface sites, As will displace P by a 50 to 1 ratio. Therefore, the epitaxial surface must have an arsenic surface coverage depleted of As, so as to allow for P incorporation. Thus, the As/(In+Ga) ratio is controlled, and phosphorus is the remaining constituent species which is in abundance and primarily sets the Group V to Group III overpressure.

The control algorithm for the alloy composition is initiated by establishing the In/Ga ratio which will determine the bandgap of the alloy. By modifying the As content, the $In_{1-x}Ga_xAs_yP_{1-y}$ alloy is lattice-matched to the InP substrate. This control algorithm allows for variation of the energy bandgap, while maintaining the lattice match to InP.

Figure 8a shows an (In,Ga)(As,P)/InP rib waveguide design that has been optimized for both maximum coupling to a Bragg grating (not shown) and for minimum fabrication-induced waveguide loss. (The Bragg grating will be etched on the top of the rib.) The 200 Å quaternary layer provides an etch stop for the fabrication process, to enable the height of the waveguide rib to be well defined and repeatable from sample to sample. Figure 8b is a SEM micrograph of a waveguide facet that was stained to enhance the contrast between epitaxial layers. In a parallel effort, the masks necessary to characterize the waveguides have been designed and manufactured with emphasis on the study of waveguide loss, as measured by cutback and Fabry-Perot techniques, waveguide-waveguide coupling, and facet reflectivity of waveguides angled with respect to the cleaved end.

Thesis

Damask, J.N. *A New Photonic Device: The Integrated Resonant Channel-Dropping Filter.* S.M. thesis, Dept. of Electr. Eng. and Comput. Sci., MIT, 1993.

3.5 Heterovalent Interfaces Composed of II-VI/III-V Heterostructures

Sponsor

National Science Foundation
Contract DMR 92-02957
Grant DMR 90-22933

Project Staff

Professor Leslie A. Kolodziejski, Dr. Gale S. Petrich, Jody L. House, Kuo-Yi Lim

Epitaxial growth of the wide bandgap semiconductor ZnSe onto GaAs buffer layers is complicated by the disparity between the electronic configuration which exists during the formation of the heterointerface. Due to the change in valency occurring from one monolayer to the next as the II-VI/III-V interface is formed, interface states are generated at the heterointerface. The interface states affect the efficiency of the carriers being injected from the GaAs to the ZnSe (for example in a pn diode configuration). One method for investigating the nature of the interface states in the ZnSe-on-GaAs "noninverted" heterostructure is through the examination of the electrical characteristics of depletion-mode MISFET devices, where ZnSe is the insulator for the GaAs channel. Modification of the density of interface states will be studied by engineering the stoichiometry of each layer during the interface formation. The fabrication of the ZnSe/GaAs MISFET devices involves the development of the wet etch and ohmic metallization techniques, in addition to the creation of an appropriately designed device mask set. The masks have been designed so that the gate lengths range from 2 to 50 microns. Currently, the growth parameters and the processing steps for the ZnSe/GaAs heterostructure are under development.

The fabrication of the inverted interface, i.e., GaAs-on-ZnSe, for the fabrication of multilayered structures composed of ZnSe wide bandgap barriers and GaAs quantum well layers, represents a challenge in materials science. The growth approach must address issues regarding materials which are fabricated at vastly different growth temperatures (the optimum growth temperatures differ by almost 300°C). The first effort toward fabrication of the inverted structure has been to examine the
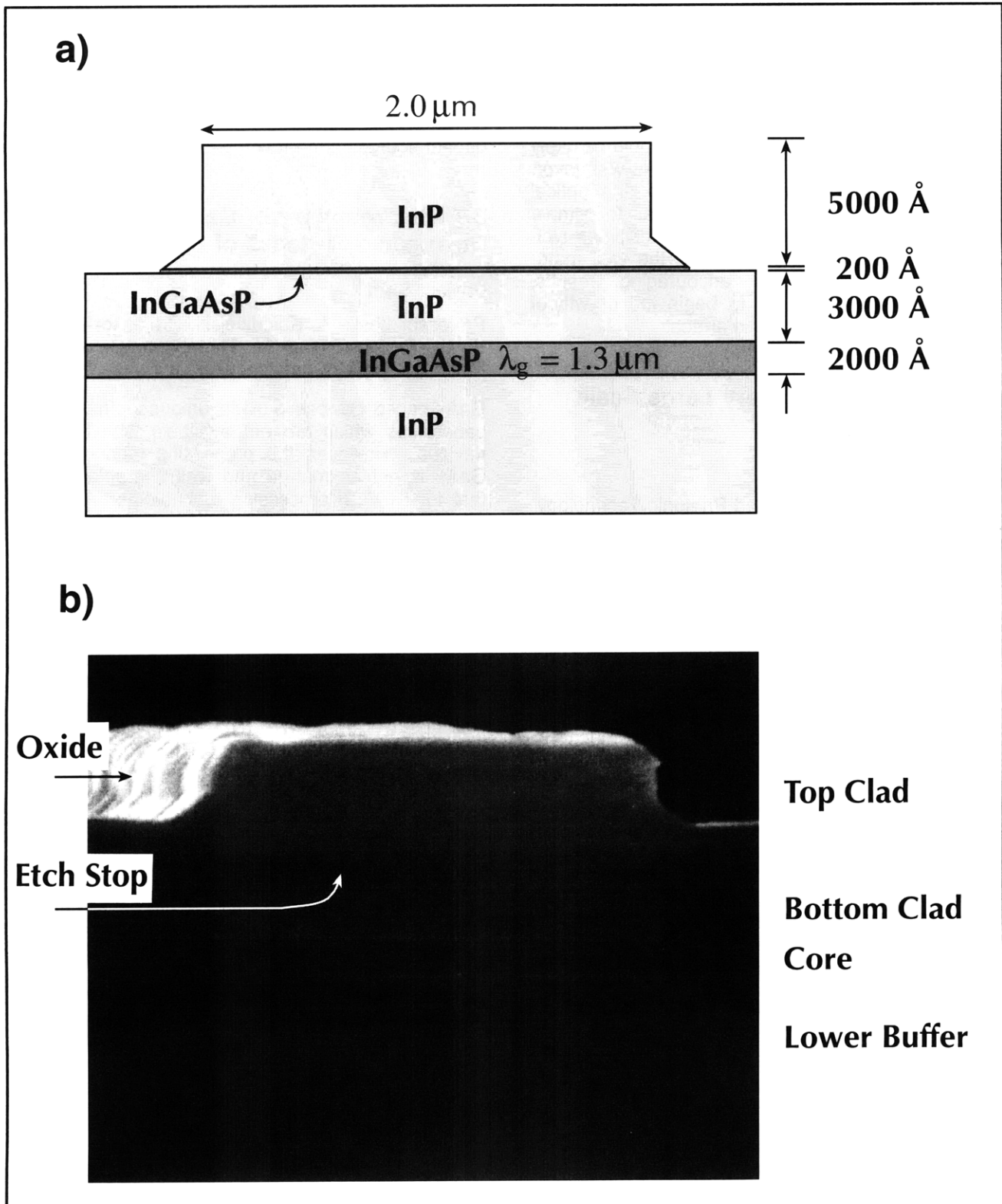
a)

2.0 μm

InP — 5000 Å

InGaAsP — 200 Å

InP — 3000 Å

InGaAsP $\lambda_g = 1.3\,\mu m$ — 2000 Å

InP

b)

Oxide

Etch Stop

Top Clad

Bottom Clad

Core

Lower Buffer

Figure 8. A cross sectional view of the (In,Ga)(As,P)/InP rib waveguide. (a) The designed structure showing the individual layers and thicknesses. The 200 Å quaternary layer provides an etch stop for the waveguide. (b) A SEM micrograph of the InP/(In,Ga)(As,P)/InP waveguide structure.

effects of very low growth temperatures on the GaAs layers, as characterized by high resolution x-ray diffraction and photoluminescence. Only at the very lowest growth temperature (~ 270°C) is excess As incorporation observed. In addition, ZnSe layers (grown on GaAs) have been subjected to various temperature extremes, as would be likely to occur during the growth of the GaAs well layer. As determined by photoluminescence, the optical properties of the ZnSe layers appear to remain unaffected by rapid thermal anneals, for times typically encountered during growth of the well material. With these two encouraging results, experiments are underway to begin the growth of the inverted GaAs-on-ZnSe interface.

3.6 Optoelectronic Very Large Scale Integrated Circuits

Sponsor

National Center for Integrated Photonic Technology
Contract 542-381

Project Staff

Professor Clifton G. Fonstad, Jr., Professor Leslie A. Kolodziejski, Dr. Gale S. Petrich, Joseph F. Ahadian, Kan Lu

The project described herein has as an objective the development of Al-free compound semiconductor lasers for commercially viable OptoElectronic VLSI circuit (OE-VLSI) technology. The lasers which are being fabricated will eventually be regrown onto commerially fabricated GaAs MESFET VLSI circuits. These fully metallized VLSI circuits have previously been found to withstand temperatures of up to 500°C for several hours without degradation. Conventionally-grown (Al,Ga)As-based lasers require growth temperatures greater than 600°C to achieve high quality material, and therefore will not allow for regrowth onto the completed VLSI circuitry. In contrast, however, the (In,Ga)(As,P) heterostructure system is normally grown at substrate temperatures near or below 500°C. At present, multiple quantum well (In,Ga)As/GaAs/(In,Ga)P laser structures have been designed. High quality (In,Ga)P epilayers on GaAs substrates have been deposited, and both n- and p-type doping studies are underway to calibrate the dopant sources and growth parameters.

3.7 Heteroepitaxy of GaAs onto Corrugated Surfaces of Si

Project Staff

Professor Leslie A. Kolodziejski, Professor Henry I. Smith, Professor Carl V. Thompson, Dr. Gale S. Petrich, Sean M. Donovan, Kan Lu

GaAs-based devices provide unique optoelectronic capabilities which are not available with Si-based devices. However, the processing technology for GaAs is not as mature and well characterized as that for Si VLSI processing technology. A natural step would be to combine the two device systems via monolithic integration, which requires the heteroepitaxial growth of GaAs onto Si. A significant obstacle, however, occurs due to the 4.1 percent lattice mismatch, and the presence of large differences in thermal expansion coefficients between the two materials giving rise to unacceptably high dislocation densities in the GaAs overlayer. In earlier work by Professor Smith and coworkers,[14] it was observed that by etching a silicon substrate to contain a saw-tooth-like pattern that the threading dislocation density in the surface regions of a heteroepitaxially-grown GaAs film was greatly reduced. A detailed investigation is underway in order to understand the mechanism responsible for the reduction in the dislocation density, which will result in the successful integration of GaAs and Si functionalities. The study will also aid in the understanding of polar on non-polar epitaxy using GaAs-on-Si as the test structure. Our work thus far has primarily emphasized refinement of the process for producing the saw-tooth patterned Si substrates and preparing the surface for GaAs epitaxy.

---

[14] K. Ismail, F. Legoues, N.H. Karam, J. Carter, and H.I. Smith, "High-quality GaAs on Sawtooth-Patterned Si Substrates," *Appl. Phys. Lett.* 59: 2418-2420 (1991).